A review of Sensorless Control in Induction Machines using HF Injection and Test Vectors

Cyril Spiteri Staines, Cedric Caruana, Nicholas Teske, and Joseph Cilia

Department of Electrical Power and Control,
Faculty of Engineering, University of Malta, MALTA
URL: http://www.eng.um.edu.mt

Abstract - **This paper describes various methods aimed at tracking the flux and rotor position for cage induction machines without a shaft sensor using specially designed saliencies or natural saliencies. The estimation methods employ a High Frequency (HF) signal or test vectors to detect the machine saliency. As is common knowledge, multiple saliences can cause problems to track only one particular saliency. Ways to overcome this problem for rotor position and rotor flux tracking are discussed. The performance of these methods is investigated at all loads at low and zero speed and also at zero fundamental frequency.**

I. INTRODUCTION

Model based speed estimation in AC machines is possible at nearly all speeds, however most methods fail at low or zero speed. The reason is that speed estimation fundamentally depends on the determination of the back-*emf* or the machine flux. At low speed, the back-*emf* decreases to an extent that inaccuracies in sampled variables and inexact knowledge of the machine parameters yield relatively large estimation errors. In this respect, recent research was aimed at estimating the rotor, or airgap-flux position, using a method, which is independent of machine and inverter parameters. By tracking some form of saliency in the machine, the flux or rotor position can be estimated at zero and low speeds. Saliency detection methods can be of three types : transient, h.f. bursts and continuous signals.

One technique is the INFORM method [3,14], which estimates the flux angle by applying a transient test voltage and calculating the leakage inductance which varies due to the main path and leakage (slot) saturation. Another transient technique for rotor position tracking by measuring the zero-sequence voltage response to a sequence of test vectors was developed in [6,23]. This method was applied to a star connected induction machine (IM) exhibiting a high rotor slotting effect. The method was then developed for delta connected cage machines [21,24], where the resulting zero-sequence current derivatives were used for rotor flux position tracking. Methods using a continuous HF voltage injection require an observer for saliency tracking. The machine saliency will create rotor or flux position-dependent harmonics in the HF stator currents which can be signal-processed to yield the required position. The observer can be configured to track magnetic flux [7,8] or physical saliencies [1,11,17,22].

Rotor "flux tracking" approaches yield parameter-independent flux position. These methods will give good low-speed torque and flux control if the machine is sufficiently saturated. In particular the rotor perimeter and slot bridges need to be saturated; open slot rotors are therefore less suitable. For sensorless position and speed control at zero and low speeds a 'trackable' rotor position dependent saliency is required. This can be the natural saliency due to rotor slotting [6,16,17,18] or a designed rotor asymmetry [1,7]. Rotor position detection is successful at low loads and reduced flux. Main flux and the leakage flux saturation will cause another saturation saliency-dependent HF harmonic in addition to that of the rotor asymmetry. The multiple saliencies so created can lead to erroneous rotor position tracking. For successful rotor position estimation, either:

(i) the rotor asymmetry needs to be designed in such a manner so as to yield a position-dependent harmonic which under all operating conditions is larger than the other HF saliency harmonics, or

(ii) the estimation method has got to be capable of taking into account multiple saliency effects.

The first solution is only possible by designing a high degree of engineered saliency into the rotor [1]. Unfortunately this influences the machine torque output. The second solution can be carried out by compensating for the saturation-dependent HF harmonic by using HF magnetising curves [11] or by using a different HF injection strategy [2] or using a multiple saliency model in the estimator [13].

This paper discusses rotor position and rotor flux position tracking yielding sensorless torque, speed and position control using three types of rotors:

Type A: 30kW double cage machine with designed outer cage rotor resistance asymmetry [1]. By implementation of a sinusoidal variation over one pole pitch of the rotor outer cage resistance for a double cage IM. (Rotor resistance asymmetry was designed to be $R^r_{r1\alpha} = 0.98\Omega, R^r_{r1\beta} = 9.98\Omega$.)

Type B: 30kW machines exhibiting rotor slotting. These machines are generally open or semi-closed slot and the optimum rotor slot number can be selected from the criteria in [12]. (Type B machine uses a near-standard industrial rotor with $N_r=56$ unskewed rotor slots [17]). In type A and B, the rotor flux position and/or the rotor position may be derived.

Type C: 11kW 'off–the–shelf' closed slot machine exhibiting small or negligible slotting effects. These machines are generally skewed, closed slot with stator-rotor slot numbers selected to minimize slot ripple. For such machines injection technique will yield the position of a "saturation" vector from which the rotor flux vector only can be derived.

II. Continuous HF Injection for Tracking Rotor Position Saliencies

If the injected HF carrier voltage is :

$$v^s_{s\alpha\beta\_c}(t) = V_c e^{j\omega_c t} \tag{1}$$

The resulting HF stator currents including saturation-dependent harmonics will be [10]:

$$i^s_{s\alpha\beta\_c}(t) = I_1 e^{j(\omega_c t+\phi_1)} + I_2 e^{j(2\theta_r-\omega_c t-\phi_2)} + I_3 e^{j(2\theta_e-\omega_c t-\phi_3)} \tag{2}$$

Using the currents of equation (2) (assuming that I3 =0) for the scheme shown in fig. 3, after the harmonics at frequency $2f_e$ are filtered off, t can be shown [10] that a form of linear error is obtained:

$$\xi_f = I_2 \sin\left(2(\theta_r - \hat{\theta}_r) - \phi_2\right) \tag{3}$$

For this error to go to zero, we can write:

$$2(\theta_r - \hat{\theta}_r) - \phi_2 \approx 0 \text{ and, } \hat{\theta}_r \approx \theta_r - \frac{\phi_2}{2}.$$

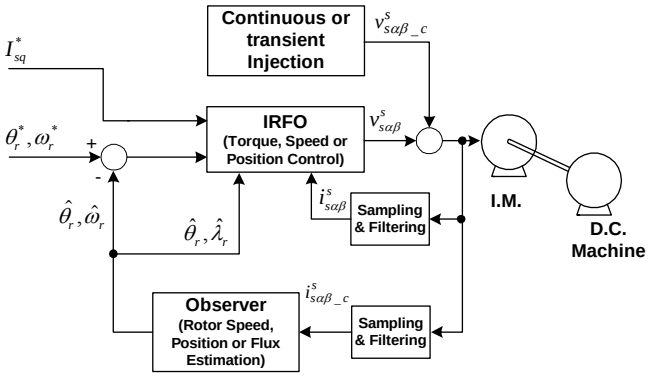

Figure 1. Basic Sensorless Torque, Position or Speed Control System.

A. Continuous HF injection for tracking Rotor Position Saliency.

The control structure of fig. 1 with Type A machine was used. An indirect rotor flux orientation (IRFO) scheme was used both for speed or position control. A high frequency voltage injection of about 300Hz was superimposed over the fundamental frequency. The resulting HF current magnitude was about 7% of the rated main excitation current. Fig. 2. shows the structure to resolve the position and speed. The resulting stator HF current obtained under sensored speed control with a demand of 600 rpm is shown in fig.3.

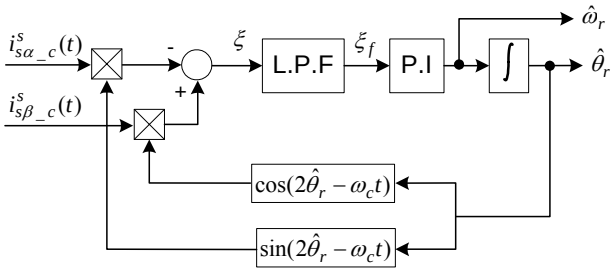

Figure 2. A closed-loop position and velocity PLL using phase detector based on the heterodyning technique.

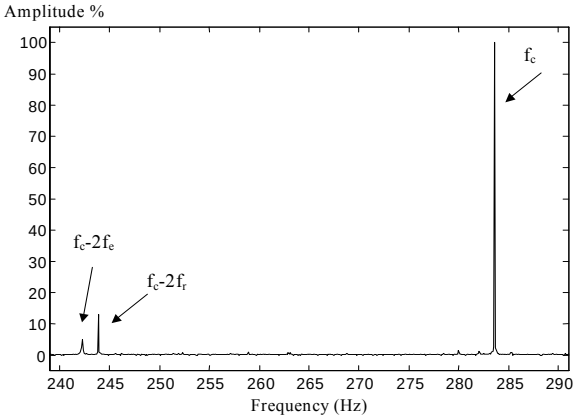

Figure 3. HF Current Spectrum at 600 rpm and 50% load.

The system of fig. 1 was used for sensorless position control. Fig. 4. shows the step response to a position demand of 360 mechanical degrees during 50% rated load respectively. The system becomes susceptible to a low frequency oscillation which worsens once the load is increased beyond 50%. The oscillations are due to the saturation-induced HF harmonics (f_c-$2f_e$).

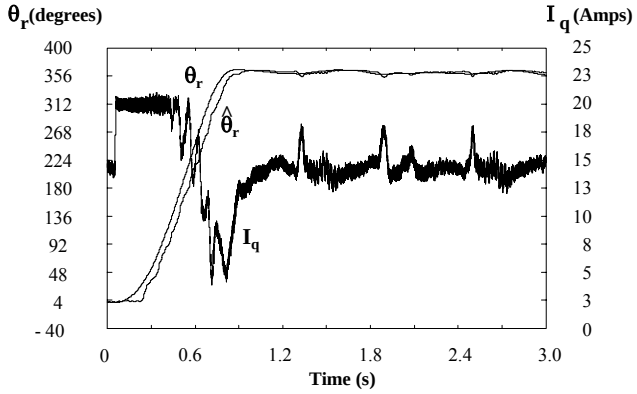

Figure 4. Sensorless position response to a transient demand of 360º (50% rated load.)

B. Suppression of the Saturation Harmonics

A possible solution to suppress the deteriorating effect of the saturation-dependent HF harmonics (at $2f_e$ and multiples) is to implement a compensation scheme [11] using the structure of fig. 5. If only one saliency is present, the output negative sequence signal $i^s_{sdq\_c}$ will then contain the *sin* and *cos* of the position angle. In practice however there will be additional parasitic saliencies together with the dominant saliency. The *Harmonic Compensation* (HC) technique [11] can be applied to remove distorting or unwanted harmonics. The HC has been shown to be effective if only a small number of harmonics have to be suppressed. An automated commissioning will determine these 'un-desired' harmonics (magnitude i_{C1}, phase φ_{C1} and frequency) as a function of the operating point (i_{sd}, i_{sq}) and the stator current angle θ_e.

$$\hat{i}_{C1} = f(i_{sd}, i_{sq}) \tag{4}$$

$$\hat{\theta}_{C1} = f(i_{sd}, i_{sq}, \theta_e) \approx 2\theta_e + \hat{\varphi}_{C1} \tag{5}$$

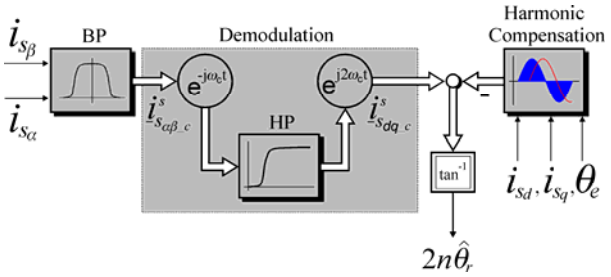

Figure 5. Structure for demodulation and transformation of negative sequence harmonics.

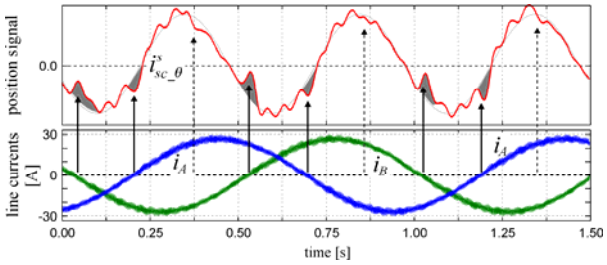

Figure 6. **Top:** Discrete distortion of position signal $i^s_{sc\_c}$ after HC, for asymmetric machine (Type A, harmonic at $2f_r$). **Bottom:** line currents.

C. Suppression of the Inverter Modulation Harmonics

If the available rotor saliency is small, the inverter non-linearity can introduce significant distortions in the HF signals. Fig. 6. shows the distortion (grey areas) in the demodulated negative sequence signal in Type A machine driven from a 45kW inverter after applying HC in the time-domain. The distortion is most pronounced at the time of the zero crossing of the line currents. Fig. 7. shows the frequency spectrum of the position signal for Type B machine before any compensation is applied. The inverter-modulation harmonics are a multiple of the excitation frequency f_e. and depend on the operating condition. The shorter the zero crossing, the smaller the distortion. The inverter distortion therefore decreases with speed or load. If a larger dead-time cannot be avoided, a dead-time compensation scheme may be implemented.

A second possibility for improving the position estimate is to implement a compensation strategy that suppresses the HF inverter modulation via signal processing [18]. *Space Modulation Profiling* (SMP) was developed and carries out real-time compensation using a pre-determined envelope of the 'un-desired' harmonic distortion signals (multiples of the fundamental frequency). The harmonics due to the saturation saliency and the inverter distortions are removed from the demodulated HF currents using pre-loaded profile of for the direct position signal axis and a similar profile for the quadrature axis. The profile is recorded for rated flux and different load over the stator current angle.

D. Results of HC and SMP Techniques

The drive was connected as shown in Fig. 1 together with the rotor position estimator of fig.5, where either HC or SMP can be used. The estimated rotor position was used for field orientation and serves as the feedback to the position controller. The position controller is a lead controller. A dc machine is attached to the shaft of the IM and acts as load. The rotor position tracking and sensorless position control was tested using different induction machines under full flux and all loads. The first experimental results are taken using a delta-connected Type A induction machine. The saturation saliency is suppressed using the HC technique. The inverter modulation suppression (SMP) was not used.

Fig. 8. shows a fast position transient of the sensorless drive when the rotor position is changed by *360* degrees mechanical, while the load is at *80%* rated. The machine is fully fluxed. The position change is performed in less than *0.7* seconds. The upper plot of fig. 8 shows the real and estimated rotor position. Below are the vector currents i_{sd} and i_{sq}. During this experiment, the i_{sq} current limit was set to *36*A to deliver the high load torque and the additional transient torque.

The second machine tested is the delta-connected Type B machine. The saliency due to the rotor slots is used for position estimation. A suppression of the inverter modulation was necessary to make sensorless control possible. The SMP is applied to suppress saturation and inverter modulation, combined with the demodulation of fig. 5.

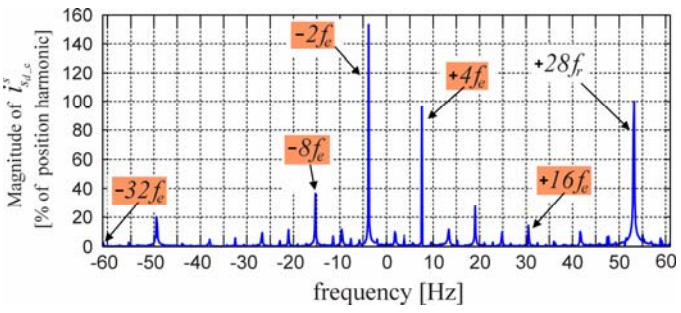

Figure 7. Spectrum of the demodulated position signal $i^s_{sd\_c}$ for symmetric machine (Type B) with slotting saliency harmonic at $28f_r$.

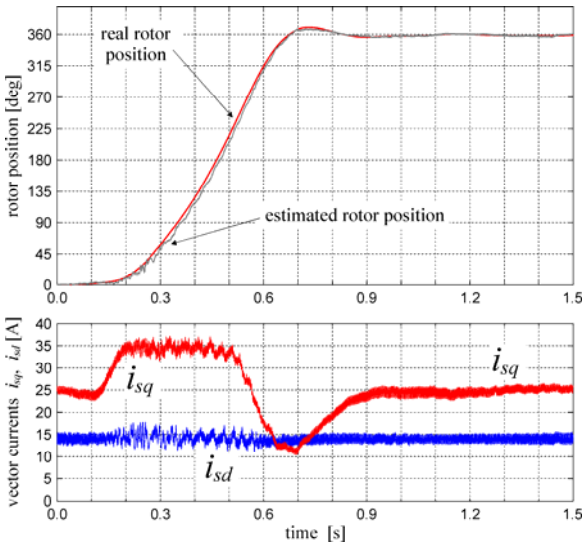

Figure 8. Sensorless position change by one revolution for asymmetric machine. *Top*: real and estimated rotor position. *Bottom*: vector currents.

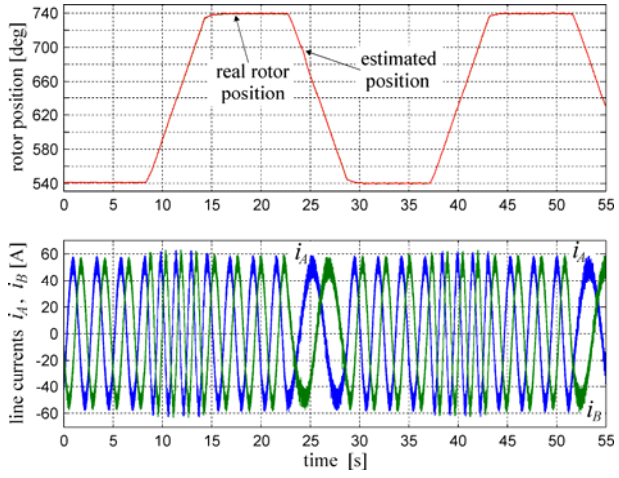

Figure 9. Sensorless position control using the symmetric machine under 65% rated load. **Top:** reference, real and estimated rotor position. **Bottom:** line currents iA and iB.

Fig. 9. shows a sequence of slow position changes by *200* degrees mechanical and position holding for the fully fluxed machine. The load is constant and at *65%* rated. During a position change, the rotor moves at a speed of *5.5rpm* and after the reversal at *–5.5rpm*. The difference between real and estimated position has an error with a standard deviation of less than *0.45* degrees mechanical for all operating conditions.

III. Continuous HF Injection for Tracking Rotor Flux Position Saliency.

For rotor flux tracking using HF injection, machines exhibiting small or negligible slotting effects should be used. Machines are generally designed to operate under saturated conditions at rated flux to better utilize the machine iron. The resulting saturation saliency, which was considered as the source of the corrupting harmonics in rotor position tracking, can be used directly for rotor flux tracking. The drive structure and the signal processing are similar to those in figures 1 and 5, only the estimated angle will be $\hat{\theta}_e$ rather than $\hat{\theta}_r$. Such schemes assume that there is a main flux already established in the machine that causes saturation in its main direction. It is also assumed that the fundamental flux linkage is not affected by the test signal as otherwise the saliency position will follow the injected signal.

There are different parts of the machine iron that will saturate and the resulting saturation pattern in the machine and hence the saturation saliency will reflect the interaction of the different fluxes in the machine, particularly when the machine is loaded. The saturation saliency will not be ideal and there will be secondary saturation space harmonics. The position signals p_α and p_β can also contain other harmonics that result from the inverter non–linearity, which coincide with the saturation saliency harmonics as discussed before. Space Modulation Profiling (SMP) is used in this work to decouple the useful $2f_e$ harmonic. The frequency spectrum of the position signals obtained on an Type C at 60r/min, 20% and 100% loads are shown in Fig. 10.

The high frequency injection schemes effectively track the change in inductance of the machine's leakage flux paths. The estimated angle $\hat{\lambda}$ will not necessarily directly reflect the rotor flux position λ_R, as the leakage paths are saturated both directly and indirectly by the main flux [8]. In addition, there are a number of localised fundamental leakage flux components that contribute to the leakage path saturation. This is a concern here, as opposed to the rotor position estimation approaches, as the absolute rather than an incremental (as for position estimation) rotor position is required for true vector control.

Fig. 11 plots the Saliency Orientation Shift (SOS) that reflects the difference $\left(\hat{\lambda} - \lambda_{R\_IRFO}\right)$ for the 11kW closed slot machine. It is suggested in [8,25] that the SOS reflects the difference between the stator and the rotor fluxes can be predicted by a simple equation. Fig 11 shows that the SOS for the experimental closed slot machine is certainly not linear.

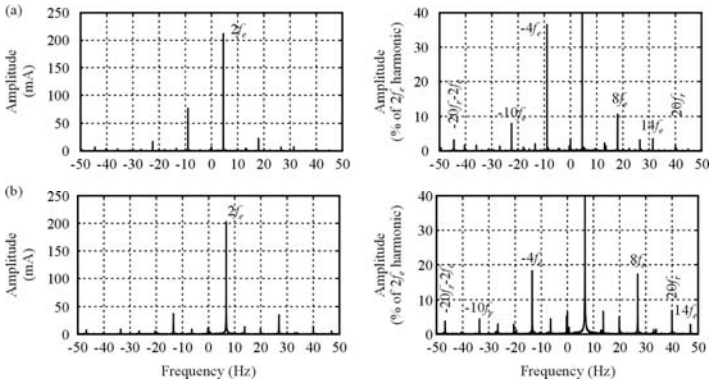

Figure 10. Harmonic Spectrum for the position signal pα under motoring conditions (a) 20% and (b) 100% rated torque at 60r/min.

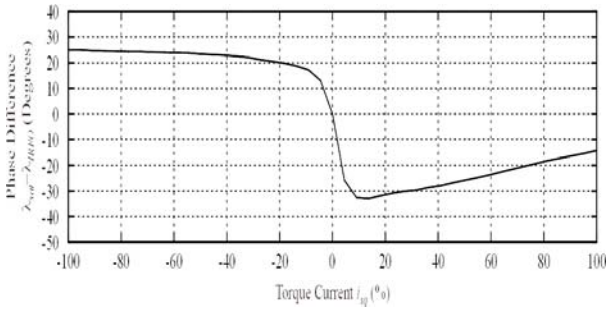

Figure 11. Saliency Orientation Shift (SOS) characteristic for the experimental 11kW closed slot induction machine.

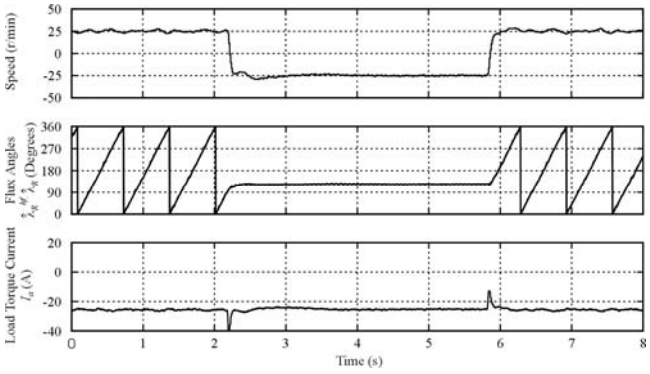

Figure 12. Sensorless torque control with induction machine supplying torque at zero frequency under regenerative conditions: -24r/min at 65% torque.

The experimental tests are done on a test rig consisting of a 4–pole, delta connected, off–the–shelf induction machine with closed slots and skewed rotor. Standard dead–time compensation is implemented by advancing the ON commutation for positive line current and the OFF commutation for negative line current [25]. The final estimated angle for sensorless torque control is obtained from a hybrid system where the angle derived from the hf injection $\hat{\lambda}_R^{hf}$, after SMP and SOS compensation, is used to force the output of a "voltage model" observer.

The performance of the system is shown in Fig 12, where the induction machine is at a constant 65% torque reference when the speed toggles between ±24 r/min such that the excitation frequency f_e of the induction machine is zero.

IV. Zero Sequence Current Derivative Method

The Zero Sequence Current Derivative (ZSCD) method of position estimation involves applying voltage test vectors corresponding to six non-zero switching states of a voltage source inverter (VSI). These test vectors are of very short duration (12-15μs) and are applied in between the normal PWM generation. The vectors are applied in pairs (V_1,V_4), (V_3,V_6) and (V_5,V_2) during the PWM generation [21]. The applied vector pairs are equal and opposite and will have no effect on the fundamental excitation of the IM. Each time a test voltage vector is applied, corresponding currents will flow in each phase of the IM, including the zero sequence component whose derivative may be measured by a single non-integrating Rogowski coil.

For an IM it can be shown that the stator leakage inductance, l_σ varies sinusoidally with respect to both the flux and rotor angle under the effects of main-flux/tooth saturation and rotor slotting respectively, we have:

$$l_{s\sigma\_x} = l_{s\sigma} - \Delta l_{s\sigma\_sat}\cos(2\omega_e t - k.2\pi/3) - \Delta l_{s\sigma\_RS}\cos(n\omega_r t - k.2\pi/3 + \phi) \quad (6)$$

where phase 'x' corresponds to phase a,c,b for k=0,1,2 respectively. $l_{s\sigma}$ is the average inductance per phase and $\Delta l_{s\sigma\_sat}$ and $\Delta l_{s\sigma\_RS}$ are the change in leakage inductance caused by saturation and rotor slotting respectively. The rotor slot frequency is a multiple of the rotor frequency given by; $n = Nr/pp$, where Nr is the number of rotor slots and pp is the pole pair number, and ϕ is an arbitrary phase angle.

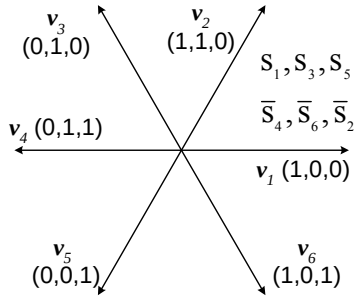

Figure 13. S1,S2,S3 correspond to the swithcing state of leg 1,2,3 of an inverter.

To detect the change in inductance, the test voltage vector pairs, (V_1,V_4), (V_3,V_6) and (V_5,V_2) corresponding to fig. 13 are applied over successive PWM cycles. For a delta-connected machine the ZSC is given by:

$$i_{s\_0} = i_{s\_ab} + i_{s\_bc} + i_{s\_ca} \quad (7)$$

Sampling just the first or second of the test vector pair gives a three phase system of "position" signals:

$$p_a = \frac{di_{s\_0}^{1}}{dt} or \frac{di_{s\_0}^{4}}{dt} \qquad p_b = \frac{di_{s\_0}^{3}}{dt} or \frac{di_{s\_0}^{6}}{dt}$$
$$p_c = \frac{di_{s\_0}^{5}}{dt} or \frac{di_{s\_0}^{2}}{dt} \quad (8)$$

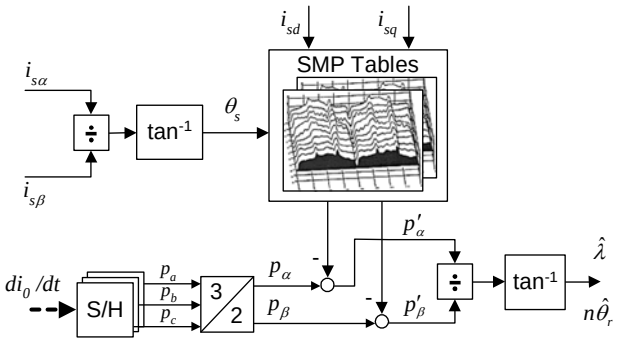

Figure 14. Basic ZSCD Flux/Rotor Position Estimation System

where:

$$p_a = \Delta l_{s\sigma\_sat}\cos(2\omega_e t - 4\pi/3) + \Delta l_{s\sigma\_RS}\cos(n\omega_r t - 4\pi/3 + \phi)$$
$$p_b = \Delta l_{s\sigma\_sat}\cos(2\omega_e t - 2\pi/3) + \Delta l_{s\sigma\_RS}\cos(n\omega_r t - 2\pi/3 + \phi)$$
$$p_c = (\Delta l_{s\sigma\_sat}\cos(2\omega_e t) + \Delta l_{s\sigma\_RS}\cos(n\omega_r t + \phi) \quad (9)$$

where the amplitude A is proportional to the dc link voltage.

Equation (9) represents a three phase system of flux and rotor angle dependent signals. The sampled 3-phase signals (p_a, p_b, p_c) are transformed to a 2-phase system (p_α, p_β). The first terms, ($\Delta l_{s\sigma\_sat}$), are dependent on machine saturation whilst the second terms,($\Delta l_{s\sigma\_RS}$) are dependent on rotor slotting and contain the 'rotor position dependent' information. It is noted that (9) is ideal; in practice harmonics of the saturation component $2k\omega_e$, k = 2,3,…, will exist arising from non-linear converter effects, saturation space harmonics [18] and high order terms arising from the binomial expansion used in the derivation of (6).

A. Harmonic Separation

The separation of the different harmonic components of (9) cannot be done using real-time filtering. The method used in is that of the Space Modulation Profile (SMP). This can be used for obtaining clean positions signals for both flux position and rotor position estimation. Fig. 14 depicts the basic configuration of the SMP memory compensation to obtain clean position signals. The compensation terms depend on the actual torque current (i_q), the field current (i_d) and the stator current vector angle (θ_s). After correction of the position dependent signals (p_α and p_β), their argument is used for the rotor flux or the rotor position estimate:

$$\text{Rotor Flux Estimate: } \hat{\lambda} = \tan^{-1}\left(\frac{p'_\beta}{p'_\alpha}\right) \quad (10)$$

$$\text{Rotor Position Estimate: } n\hat{\vartheta}_r = \tan^{-1}\left(\frac{p'_\beta}{p'_\alpha}\right) \quad (11)$$

B. Sensorless torque control (rotor flux angle tracking)

In these experimental results, the Type C machine was used under torque control. Equation (10) and an *Saliency Orientation Shift* (SOS) scheme were used to track the flux angle. The estimated angle was used for supplying the vector transformations to the rotor orientated *dq* frame. The machine was torque controlled with standard i_{dq} current loops. The IM is connected to a speed controlled DC machine whose armature current i_a is monitored.

Fig. 15 shows the response to a step speed change of ±30rpm in the DC machine at the rated IM torque. Examination of the DC armature current illustrates good field orientation performance.

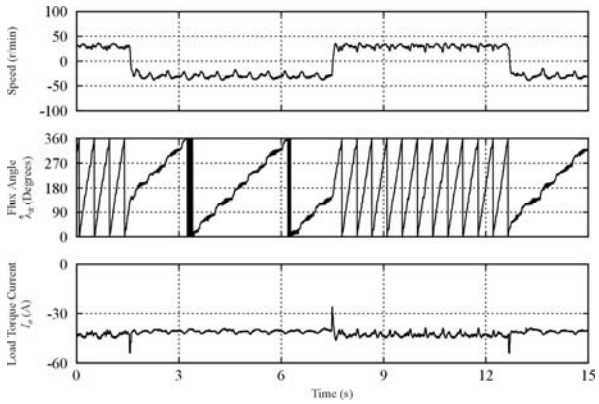

Figure 15. Sensorless torque control: speed transients ± 30rpm IM I_{sq} (ref) 100%. **Top:** Drive speed (rpm). Middle: Estimated flux angle (deg.). **Bottom:** DC machine current (Amps).

C. Sensorless speed control

In the following experimental results, Type B machine was used under speed control in which the estimated rotor position angle from (11) was directly used for the dq axis transformations under a standard IRFO control structure. The estimated angle was of such good quality that position control under no load and under loaded conditions was successful. However in this paper only the results pertaining to the more critical sensorless speed control are published. The estimated angle is also used as feedback for the speed loops. A DC machine was used to load the IM. The inverter available to drive Type B machine allowed maximum loading of 40% rated load. A low pass filter of 8Hz is applied to the differentiated rotor position estimate to provide the speed feedback.

Fig. 16 and 17 show the response of sensorless speed control to step inputs for demands of zero and low speed operation under 40% rated load. In Fig. 17, displays the estimated and actual rotor angle. The maximum position error obtained is ±1.5° and ±0.5° (mechanical) under transient and steady state conditions respectively.

Fig. 18 and 19 show the performance of the sensorless speed control system to a ramp in speed demand of 60 rpm in 0.24s. This will achieve a 's-curve' position transient of 95 mechanical degrees for a given inertia.

V. CONCLUSIONS

This paper has shown successful sensorless speed, position and torque control of induction machines by saliency tracking using continuous HF injection or test vectors. Continuous HF injection results have demonstrated operation for fully fluxed machines under high and changing loads and for zero and low speeds. In the case of the Type B machine the control of the rotor position is currently better than one degree mechanical. The distortion under high load introduced by the saturation saliency can be suppressed using the *Harmonic Compensation* or the *Space Modulation Profiling* techniques. However, acceleration and speed can be a limiting factor. The latter can be overcome by switching over to a back-*emf* model-based estimator. Good results have been obtained for reasonably fast position control and for sudden load changes.

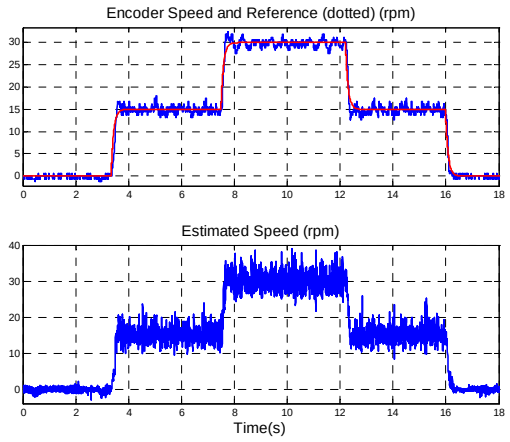

Figure 16. Speed and angle position estimation for sensorless 0 -15 -30 rpm steps under change to and show 'Isq' 40% rated load. **Top:** Encoder speed & Ref. (rpm). **Bottom:** Estimated speed (rpm).

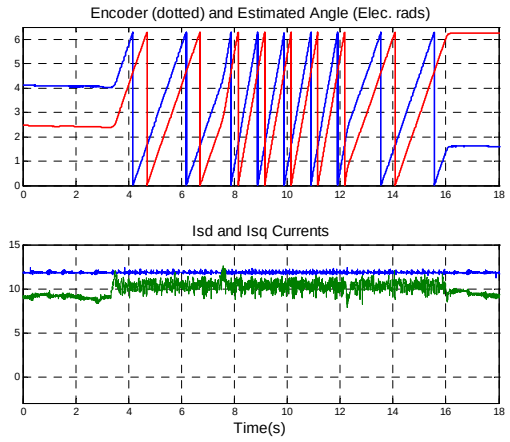

Figure 17. Position estimation and dq-currents for condition of fig. 16). **Top:** Encoder and Estimated Rotor Angle (elec. rads). **Bottom:** i_{sqd} currents

Rotor flux tracking using HF injection was used for sensorless torque control of Type C machine. The HF injection was supplemented by harmonic and SOS compensation. Although this technique outperforms observer–based methods at low frequencies, it exhibited some instability without hybrid model assistance. The cause is not understood; it may lie in the SOS curve that may induce unstable dynamic interactions between $\Delta\lambda_{IRFO}$ and $\Delta\lambda_{shift}$.

Results of voltage test vector injection coupled with ZSCD measurements show that this method provides an excellent technique for the sensorless control of delta-connected cage machines. The estimation method requires a single transducer, which provides an elegant solution given the likelihood of increased future application of integrated drive solutions.

The ZSCD technique was applied to two types of machines, one an off-the-shelf closed slot machine for which tracking the rotor flux position and sensorless torque control is appropriate. The other machine is chosen for its slotting behaviour – this is less standard but can allow for excellent sensorless position, speed and torque control.

For the rotor flux tracking of the Type C machine, it is found that the test vector/ZSCD approach yields good stable sensorless torque control over the full torque range. This contrasts with the performance obtained with HF injection on the same machine where, instability is sometimes observed at high loads. For the rotor position tracking for the Type B machine, experimental results have shown excellent (encoder-type accuracy) sensorless speed control. The limitations of the ZSCD are the bandwidth of the closed loop speed controller (constrained by the differentiation noise of the position signals which need to be filtered) and the maximum rotational speed which is constrained by the ZSCD sampling of the rotor slots.

This paper shows how tracking saliencies leads to good speed and position control of machines in the zero and low frequency range. Although these methods are most suitable for the low speed range, this is not be considered a limitation since model based observers can be used at higher speeds.

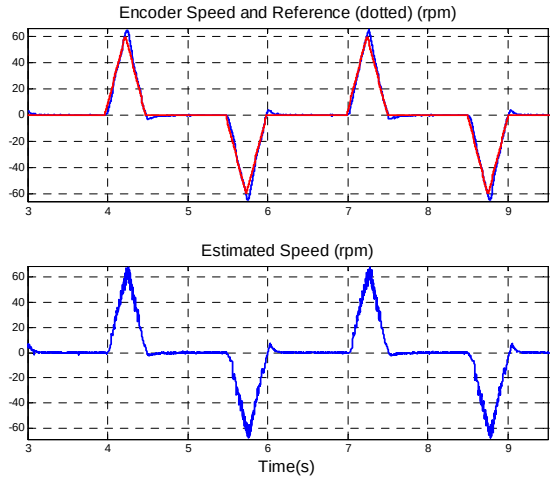

Figure 18. **Top:** Sensorless operation with Positive and Negative Speed Ramp Demand (acceleration: 250rpm /s). **Bottom :** Estimated Speed.

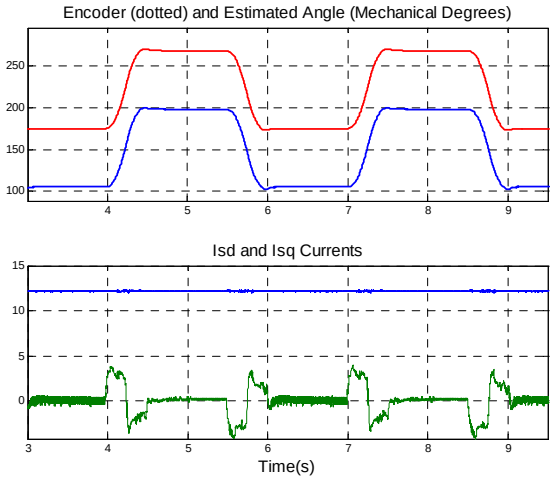

Figure 19. **Top:** Estimated and Real Position (±95º Mechanical Degrees Position Change for Speed Ramp demand of fig. 17). **Bottom:** Isd and Isq currents (Amps).

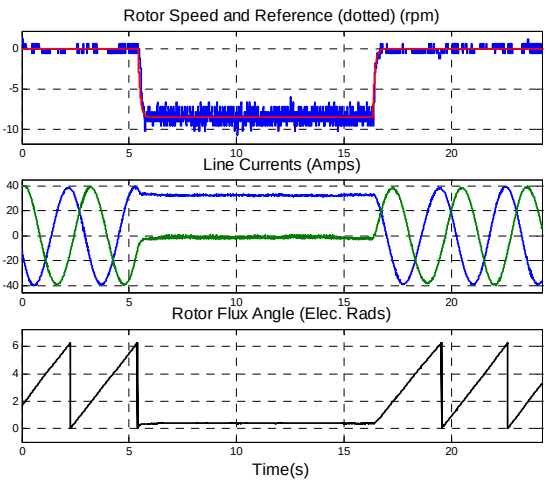

Figure 20. Sensorless Speed Control at –8.5 rpm with 40% load application reducing fundamental frequency to 0Hz. Top: Encoder Speed & Ref. (rpm). Middle:Line currents (Amps). Bottom: Rotor Flux Angle (elec. rads).

VI. REFERENCES

[1] J. Cilia, G.M. Asher, K.J. Bradley and M. Sumner, "Sensorless Position Detection for Vector Controlled Induction Motor Drives using an Asymmetric Outer-Section Cage," *IEEE Transactions on Industry Applications,* Vol. 33 No. 5, Sep/Oct 1997, pp. 1162–1169.

[2] C. Spiteri Staines, G.M. Asher and K.J. Bradley, "A Periodic Burst Injection Method for Deriving Rotor Position in Saturated Cage-Salient Induction Motors without a Shaft Encoder," *IEEE Transactions on Industry Applications,* Vol. 35 No. 4, Jul/Aug 1999, pp. 851–858.

[3] M. Schrödl, "Sensorless Control of AC Machines at Low Speed and Standstill Based on the INFORM Method," *IEEE IAS Annual Meeting, San Diego, USA, Oct. 1996*, Vol. 1 pp. 270–277.

[4] J. Ha and S. Sul, "Sensorless Field Orientation Control of an Induction Machine by High Frequency Signal Injection," *IEEE Transactions on Industry Applications,* Vol. 35, No. 1, Jan/Feb 1999, pp. 45–51.

[5] K. Ide, I. Murokita, M. Sawanura, M. Ohto, Y. Nose, J. Ha and S. Sul, "Finite Element Analysis of Sensorless Induction Machine by High Frequency Voltage Injection," *IPEC Tokyo 2000*, Vol. 4, pp. 1842-1847.

[6] J. Holtz, "Sensorless Position Control of Induction Motors – An Emerging Technology," *IEEE Transactions on Industrial Electronics*, Vol. 45, No. 6, Dec. 1998, pp. 840–852.

[7] P.L. Jansen and R.D. Lorenz, "Transducerless Position and Velocity Estimation in Induction and Salient AC Machines," *IEEE Transactions on Industry Applications,* Vol.31, No.2, pp. 240–247, March/April 1995.

[8] P.L. Jansen and R.D. Lorenz, "Transducerless Field Orientation Concepts Employing Saturation Induced Saliencies in Induction Machines," *IEEE IAS Annual Meeting,* Vol. 1, 1995, pp. 174–181.

[9] J. Cilia, G.M. Asher and K.J. Bradley, "Sensorless Position Control for Induction Motor Drives using an Asymmetric Rotor and High Frequency Injection," *Proceedings of the E.P.E. Conference, Norway*, Vol. 4, September 1997, pp. 486–491.

[10] C. Spiteri Staines, J.Cilia and G.M.Asher, "Sensorless Position Estimation in Induction Machines," *9th International Conf. On Power Electronics and Motion*, EPE-PEMC 2000, Koscie, pp6.101-6.108.

[11] N. Teske, G. M. Asher, M. Sumner, and K. J. Bradley, "Encoderless position estimation for symmetric cage induction machines under loaded conditions," *IEEE Transactions on Industrial Applications*, no. 6, vol. 37, pp. 1793-1800, Nov/Dec. 2001.

[12] Ferrah, P.J. Hogen-Laing, K.J. Bradley, G.M. Asher and M.S. Woolfson, "The Effect of Rotor Design on Sensorless Speed Estimation using Rotor Slot Harmonics Identified by Adaptive Digital Filtering using the Maximum Likelihood Approach," *IEEE IAS Annual Meeting, New Orleans*, 1997, pp. 128–135.

[13] M.W. Degner and R.D. Lorenz, "Using multiple saliencies for the estimation of flux, position, and velocity in AC machines," *IEEE Trans.Industry Applications*, vol. 34, pp. 1097–1104, Sep/Oct 1998.

[14] M. Schrödl, "Sensorless Control of AC Machines," *Fortschr.-Ber.,* VDI Reihe 21, Nr. 117, *VDI-Verlag GmbH, Düsseldorf*, 1992.

[15] F. Blaschke, J. van der Burgt and A. Vandenput, "Sensorless Direct Field Orientation at Zero Flux Frequency," *IEEE IAS Annual Meeting, San Diego, Oct. 1996*, Vol. 1, pp. 189–196.

[16] M.W. Degner and R.D. Lorenz, "Position Estimation in Induction Machines Utilizing Rotor Bar Slot Harmonics and Carrier-Frequency Signal Injection," *IEEE Transactions on Industry Applications, May/June 2000*, Vol. 36, No. 3, pp. 736–742.

[17] N. Teske, G.M. Asher, K.J. Bradley and M. Sumner, "Sensorless Position Estimation for symmetric Cage Induction Motor under Loaded Conditions," *IEEE IAS Annual Meeting, Roma, Italy, Oct. 2000*, Vol. 3 pp. 1835–1841.

[18] N. Teske, G.M. Asher, K.J. Bradley and M. Sumner, "Analysis and Suppression of Inverter Clamping Saliency in Sensorless Position Controlled Induction Machine Drives," *IEEE IAS Annual Meeting, Chicago, USA, Sept./Oct. 2001*, Vol. 4 pp. 2629–2636.

[19] C. Silva, G. M. Asher and M. Sumner, "Influence of Dead-time Compensation on Rotor Position Estimation in Surface Mounted PM Machines using HF Voltage Injection," *Power Conversion Conference (PCC)*, Osaka, Japan, April 2002.

[20] F. Briz, A. Diez and M.W. Degner, "Dynamic Operation of Carrier-Signal-Injection-Based Sensorless Direct Field-Oriented AC Drives," *IEEE Transactions on Industry Applications, Sept./Oct. 2000*, Vol. 36, No. 5, pp. 1360–1368.

[21] C. Caruana, G. M. Asher and J. Clare, "Sensorless Flux Position Estimation at Low and Zero Frequency by measuring Zero-Sequence Current in Delta Connected Cage Induction Machines", *CD-ROM, IEEE IAS Annual Meeting, Salt Lake City, 2003.*

[22] N.Teske, C.Spiteri Staines, J.Cilia and G.M.Asher, "Sensorless Position and Speed Estimation in Induction Machines", *EPE-PEMC 2002, Croatia Sep. 2002, CD-ROM.*

[23] J. Juliet, J.Holtz, "Sensorless Aquisition of the Rotor Position Angle for Induction Motors with Arbitrary Stator Windings", *IEEE IAS Annual Meeting, Seattle, Oct.3-7, 2004, CD-ROM.*

[24] Spiteri Staines, C.; Caruana, C.; Asher, G.M.; Sumner, M., "Sensorless control of induction Machines at zero and low frequency using zero sequence currents" *IEEE Transactions on Industrial Electronics*, Volume 53, Issue 1, Feb. 2006, pp: 195 – 206.

[25] J.W. Choi and S.K. Sul, "Inverter Output Voltage Synthesis using Novel Dead Time Compensation ," IEEE Transactions on Power Electronics.